Hindawi Publishing Corporation
ISRN Inorganic Chemistry
Volume 2014, Article ID 170919, 8 pages
http://dx.doi.org/10.1155/2014/170919

Research Article

Versatile SiO_2 Nanoparticles@Polymer Composites with Pragmatic Properties

Vividha Dhapte,[1] Shivajirao Kadam,[1] Varsha Pokharkar,[1] Pawan K. Khanna,[2] and Vishwas Dhapte[3]

[1] *Department of Pharmaceutics, Bharati Vidyapeeth University, Poona College of Pharmacy, Pune 411038, India*
[2] *Department of Applied Chemistry, Defense Institute of Advanced Technology (DIAT), Girinagar, Pune 411025, India*
[3] *Department of Chemistry, Bharati Vidyapeeth University, Yashwantrao Mohite College, Pune 411038, India*

Correspondence should be addressed to Vishwas Dhapte; vishwasdhapte@gmail.com

Received 17 November 2013; Accepted 10 December 2013; Published 29 January 2014

Academic Editors: A. Karadag and A. Mishra

Copyright © 2014 Vividha Dhapte et al. This is an open access article distributed under the Creative Commons Attribution License, which permits unrestricted use, distribution, and reproduction in any medium, provided the original work is properly cited.

In the present work, we report the fabrication of silica nanoparticles embedded polymeric (SiO_2 nanoparticles@polymer) composite films for numerous traits like texture, folding endurance, crystallinity, size, thermal behavior, spectral analysis, and bioactivity. Significant facets of bulky, inert, inorganic materials are known to burgeon out due to the high surface area of nanosized particles. Nature and proportion of silica nanoparticles as well as polymers exhibited remarkable impact on the fabrication and quality of casted films. Hydrophilic silica nanoparticulate-PVA films depicted better mechanical properties like thermal plus photo stability. Hydrophobic silica nanoparticulate-PMMA films showed qualities of a robust, active, thermostable, antimicrobial material that could resist extreme storage and processing conditions. Overall, these metal oxide nanoparticle-polymer composite films possess qualities reflecting their potential in food, pharmaceutical, and cosmetic industry.

1. Introduction

Presently, inorganic nanoparticulate-polymeric interfaces are evolving as intelligent approaches with miscellaneous applications. Compared to their organic counterparts, inorganic materials resist chemical attack and have good mechanical strength and higher tolerance; hence, they are explored for commercial use [1]. Cefaclor reduced gold nanoparticles coated on poly(ethyleneimine) modified glass surfaces were explored as effective and robust antimicrobial coatings for various biomedical applications [2]. Silver nanoparticles impregnated chitosan films showed fast and long-lasting antibacterial activity [3]. Magnetite nanoparticles functionalized with polymeric composites retained 100% biocidal efficiency [4]. In brief, polymeric scaffolds aid in ease of nanoparticulate fabrication and impart surface alterations along with enhanced activity [5]. Inorganic zinc oxide, titanium dioxide, and analogous metal oxides as nanoparticulate systems have received considerable attention for their exclusive features and applications [6]. As the surface area-to-volume ratio of bulk particles increases with decrease in the particle size, inorganic nanoparticles are known to illustrate miscellaneous properties leading to a plethora of activities compared to normal bulk materials. Zinc oxide nanocomposites in thermoplastic polymers showed improved interactions and immense antimicrobial activity [7]. Crack-free titanium dioxide nanoparticles casted on poly(dimethylsiloxane) substrates possessed greater antibacterial effects [8]. Silicates happen to be better inert substrates and drug carriers for chemotherapeutic agents [9]. Ciprofloxacin-loaded gold-silica core-shell nanoparticles displayed enhanced kinetics and antimicrobial efficacy [10]. Likewise, silica is used as a template to elevate biocidal efficacy of organic compounds conventionally by altering their adsorption and release patterns. However, the potential of silica nanoparticles on other substrates per se is least explored. Antimicrobial activity of SiO_2 would become more significant at nanoscale owing to increase in the surface attributes.

Table 1: Composition and physical characteristics of films.

Polymer	Ratio (polymer : SNP)	Characteristics		
		Color	Folding endurance ± SD*	Texture
PVA	20 : 1	Colorless, transparent	43 ± 0.2	Smooth
PVA	10 : 1	White, translucent	24 ± 0.1	Rough
PVA	5 : 1	White, opaque	10 ± 1.3	Rough
PMMA	20 : 1	White, opaque	24 ± 0.6	Smooth
PMMA	10 : 1	White, opaque	17 ± 0.3	Smooth
PMMA	5 : 1	White, opaque	8 ± 1.7	Smooth

*SD means standard deviation.

We herein report the fabrication of silica nanoparticles embedded polymeric (SiO_2 nanoparticles@polymer) composite films and analysis of their vital attributes for diverse applications. The effects of nature and concentration of silica nanoparticles and polymers on the biophysicochemical aspects of films are elucidated in the present work.

2. Materials and Methods

2.1. Materials. Silica nanoparticles (SNP) of 15 nm diameter were purchased from PlasmaChem GmbH, Germany. Poly(methyl methacrylate) (PMMA) and polyvinyl alcohol (PVA) were acquired from Sigma Aldrich, USA. All other chemicals and solvents used were of analytical grade, procured from Merck, India. Luria-Bertani (LB) agar purchased from Himedia Laboratories, India was used for antimicrobial studies.

2.2. Methods

2.2.1. Film Casting

Hydrophilic Films. A casting PVA solution was made by dissolving PVA in distilled water at 70°C. In the resulting solution, SNP were dispersed under vigorous stirring to form hydrophilic SNP@PVA composite films.

Hydrophobic Films. After dissolving PMMA in toluene, SNP were dispersed under vigorous stirring at room temperature to develop hydrophobic SNP@PMMA composite films.

Polymers and SNP were used in different proportions of 20 : 1, 10 : 1, and 5 : 1 (Table 1). The resulting composite mixtures were cast onto a perspex plate using casting knife and dried at room temperature for 24 hours. Perspex plates were covered with an inverted funnel for controlled evaporation. Subsequently, films were separated out and kept in the desiccators for further characterization.

2.2.2. Characterization of Films. Preliminary morphological studies were performed on prepared SNP@polymer composite films to study the effect of nature as well as proportion of polymers and SNP on the appearance and texture of films. Folding endurance was determined by folding the films of uniform cross sectional area and thickness until they break. Attenuated total reflectance (ATR) spectra were examined via Thermo Scientific Nicolet iS50R. Dried films were scanned from 600 to 4000 cm^{-1} for comparison of overlap regions and functional group identifications. Optical measurements of all films in terms of transmittance and absorbance were carried out at room temperature using UV/visible spectrophotometer (double beam JASCO V-530, Japan) in the wavelength range from 300 to 700 nm.

X-ray diffraction (XRD) patterns of dried films were recorded using an X-ray Brucker AXS diffractometer (D8 Advance, USA) with Cu line as the source of radiation. Crystallographic investigation of the films was carried out in the 2θ angle range of 10 to 80°. Average crystalline size (D) was calculated according to Debye-Scherrer's equation [11]:

$$D = \frac{K\lambda}{\beta \operatorname{Cos} \theta}, \tag{1}$$

where β is the full width at half-maximum (FWHM) intensity of a peak at an angle θ; K is the constant, depending on the line shape profile; and λ is the wave length of the X-ray source.

Surface characteristics and morphology of films were observed using scanning electron microscopic (SEM) analysis (JEOL JSM-6360A, Japan). Samples were placed on a carbon specimen holder and then coated with platinum in an auto fine coater (JEOL JFC 1600). Composition of the films was ascertained using energy dispersive analysis of X-rays (EDX) at an accelerating voltage of 20 kV and within the energy range of 0–6 keV.

Thermal behavior of dried films was measured using simultaneous thermogravimetric and differential thermal analysis (TGA/DTA) apparatus (Shimadzu, Japan) with DTG-60 detector. Heating temperature was maintained in the range of 25 to 900°C. Platinum cells were used as sample holders and flow rate of nitrogen was maintained at 50 mL/min.

Dried films were cut into fixed dimensions of 1 inch and weighed. Each film was placed in 20 mL distilled water and its weight was recorded regularly after every hour up to 24 hours. Percent water retention capacity of the film was calculated using the following formula:

$$\%\ \text{Water Retention Capacity} = \frac{(\text{Final Weight} - \text{Initial Weight})}{\text{Initial Weight}} \times 100. \tag{2}$$

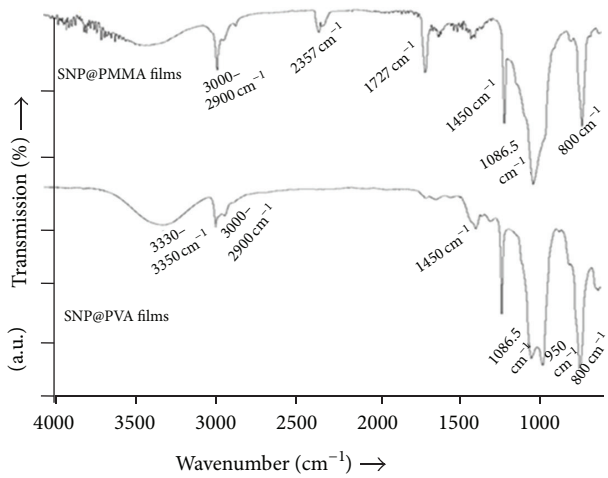

Figure 1: ATR spectra of SNP@PMMA and SNP@PVA films.

Antibacterial test was performed by film attachment method [12]. The spectrum of antibacterial activity for films was investigated on Gram-negative bacteria *Escherichia coli* (*E. coli*; ATCC number 25922) and Gram-positive bacteria *Staphylococcus aureus* (*S. aureus*; ATCC number 6538) using solid agar plate technique. LB agar (composed of NaCl 10 g/L, tryptone 10 g/L, yeast extract 5 g/L, and agar 7 g/L) plates were cultured with 10^6 colony-forming units (CFU) of each bacterial species. Hydrophilic and hydrophobic films of equal dimensions were affixed on the surface of inoculated agar plates, aseptically. Plates were incubated for 24 hours at 37 ± 2°C and evaluated for areas of inhibition.

3. Results and Discussion

In the course of present studies, different SNP@polymer composite films of general uniform thickness were cast using hydrophilic and hydrophobic polymers with SNP in 20 : 1, 10 : 1, and 5 : 1 ratios. Proportion and structure of SNP and polymers as well as their interactions portrayed the appearance and texture of prepared films (Table 1). Increasing proportion of PVA renders smooth texture to the SNP@PVA films whereas all SNP@PMMA films exhibited smooth textures. As silicon is reluctant to form multiple bonds, thermodynamically stable silica (SiO_2) needs to coordinate with additional 2 oxygen atoms [13]. PMMA with 2 oxygen atoms may suffice this intrinsic requirement of silicates easily, thereby resulting into smooth-textured films at all proportions. On the contrary, with only single oxygen atom to share, PVA may comply with SNP at higher concentrations to form smooth textured films.

The fabricated SNP@polymer composite films were studied for folding endurance (Table 1).

Folding endurance of both the films, SNP@PVA and SNP@PMMA, augmented with increase in the polymeric proportion and decrease in SNP quantity. Increasing concentration of nanosilica appends brittleness to the films. Strong interfacial interaction between the organic polymer phase and the inorganic silica phase restricted the motion of polymeric chains and hence folding endurance dropped with increase in SNP proportion [14]. Folding endurance of SNP@PVA films was greater than SNP@PMMA films due to rigid gas permeable nature of PMMA [15]. SNP@PVA (1 : 20) and SNP@PMMA (1 : 20) films with optimum physicochemical properties were opted for further analysis.

The possibility of chemical bonding between polymer and SNP was further substantiated from the ATR spectra of films. Figure 1 depicts ATR spectra of SNP@PMMA and SNP@PVA films.

Bands in the range of 3000–2900 cm^{-1} correspond to the C–H stretching of $-CH_2$. In fingerprint region of SNP@PMMA film, vibration bands at 1727 cm^{-1} (C=O) and 1450 cm^{-1} (C–O) were less intense than the vibration modes at 1086.5 cm^{-1} (asymmetric Si–O–Si stretching) [16]. This underlines the better linkage between the oxygen atoms of PMMA and SiO_2. By cross linking PVA with SNP, the characteristic –OH vibrational stretching bands (3330–3350 cm^{-1}) broaden with reduction in intensity [17]; however, the Si–O–Si stretching vibrations were noticed at the same wavenumber (1086.5 cm^{-1}). Even stretching and in-plane bending vibrations of –OH group corresponding to the molecular H_2O usually observed around 3400 cm^{-1} and 1640 cm^{-1} were absent in the ATR spectra of SNP@PVA filmThis corroborated the cross-linkage between PVA and SNP. In the SNP@PVA film spectra, bands at 800 cm^{-1} and 950 cm^{-1} (merged with 1086.5 cm^{-1}) portray symmetric Si–O–Si stretching and Si–OH flexible vibration modes, respectively, whereas the SNP@PMMA film spectra depict only the symmetric Si–O–Si stretching modes [18] due to the innate polymeric functional groups and their peculiar chemical bonding with the SNP. The characteristic band at 2357 cm^{-1} was observed for SNP@PMMA film but absent in case of SNP@PVA film. Appearance of this band suggests the impurities arising out of Si-C stretching after oxygen from the polymeric base is completely utilized [19]. Thus, PMMA binds effectively with the SNP compared to PVA.

SNP are inorganic UV-absorbing semiconductor nanomaterials [20]. Their effective binding with PVA and PMMA affects the absorbance across UV-visible range. Figure 2 shows the UV-Vis spectra of SNP@PVA and SNP@PMMA films. Absorbance spectra clearly showed absorbance wavelength at 340 ± 10 nm for SNP@PMMA and SNP@PVA films. These distinctive absorbance values in case of SNP-polymeric composite films were attributed to homogeneous distribution of SNP in the polymeric matrix. As compared to SNP@PMMA film, SNP@PVA film showed higher percent transmittance (%*T*) and lower absorbance (Abs) owing to its transparent and partially crystalline nature. Fall in the crystallinity of materials increases their band gap thus, decreasing the absorbance [21]. Thus, these films and the materials made out of them will act as ultraviolet filters to circumvent the degradation of photosensitive formulations and food spoilage or even as sun screen agents. Low %*T* and relatively higher absorbance (Abs) of SNP@PMMA film

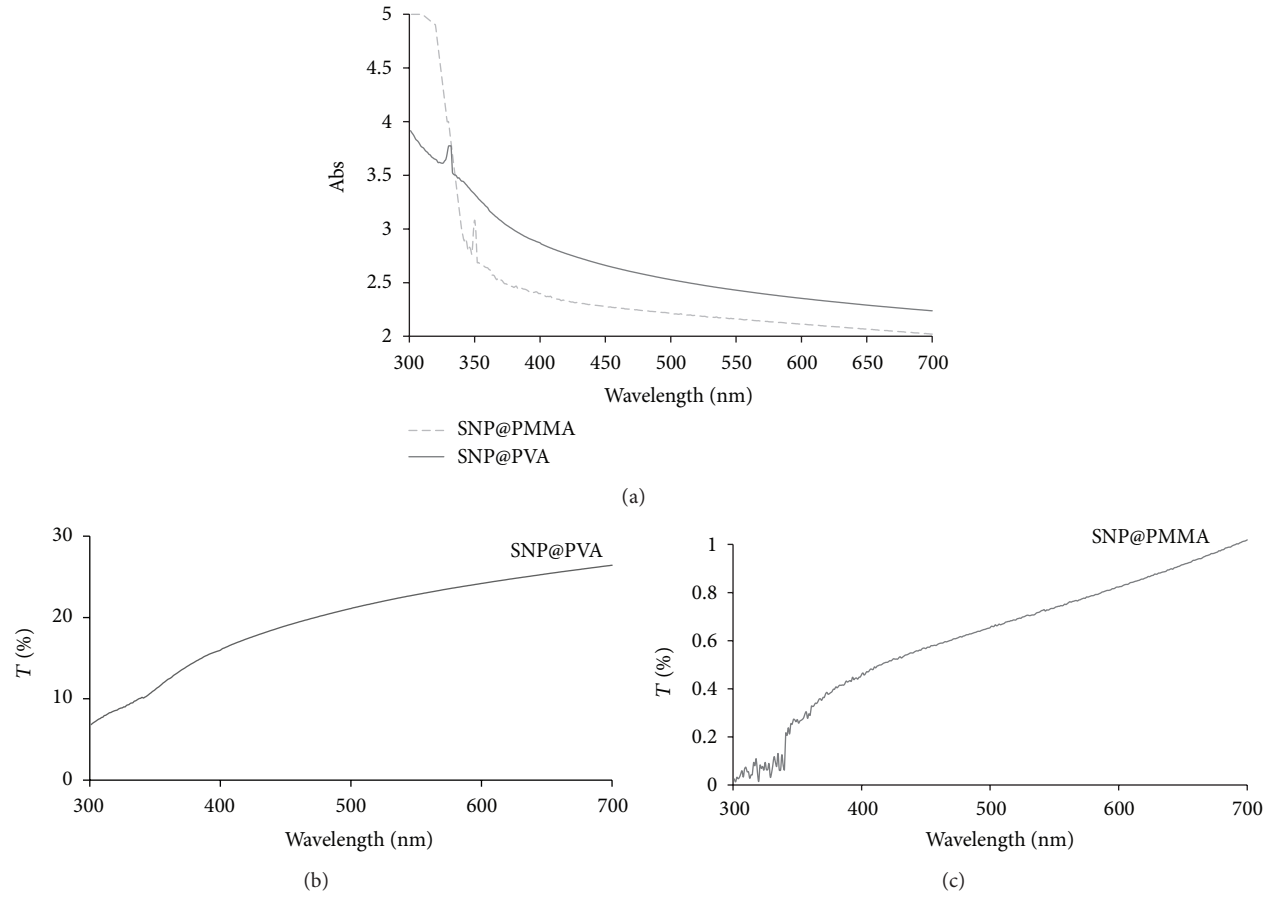

Figure 2: (a) Absorbance (Abs) and (b), (c) percent transmittance (%T) of films in the UV-Vis region.

were attributed to their opacity and crystalline properties. Such films are apt materials for drugs and products known to confront radiation sterilization during processing. All in all, SNP-polymeric composite films would form a perfect "Blockers and Absorbers" combination extending relevance towards cosmetic and topical products.

XRD spectra of SNP@PVA as well as SNP@PMMA films exhibited characteristic peaks at 2θ of 12.3° and 13.1° (Figure 3) which substantiated the presence of SNP in respective polymeric matrix. On account of the rigid gas permeable (RGP) features [15] and superior coordination chemistry with SNP, more crystallinity and hence higher intensity persisted in the SNP@PMMA film. As per the calculations using Debye-Scherrer's equation (1), the average crystalline size (D) was in the range of 14–20 nm manifesting the existence of SNP in the fabricated films.

As observed in the SEM images (Figure 4), SNP@PVA film exhibited regular morphology due to the nonagglomeration and homogeneous distribution of SNP in films. On the contrary, SNP@PMMA film indicated hazy morphology owing to its RGP features and crystallinity. EDX spectra of both films demonstrated their variable C, O, and Si composition (Figure 5). Appearance of a typical "Si" peak at 1.8 keV confirmed the successful assimilation of SNP into respective polymeric composites [9, 22]. Apparent distribution and higher composition of "Si" in SNP@PMMA film indicated efficient networking between PMMA and SNP compared to SNP@PVA film.

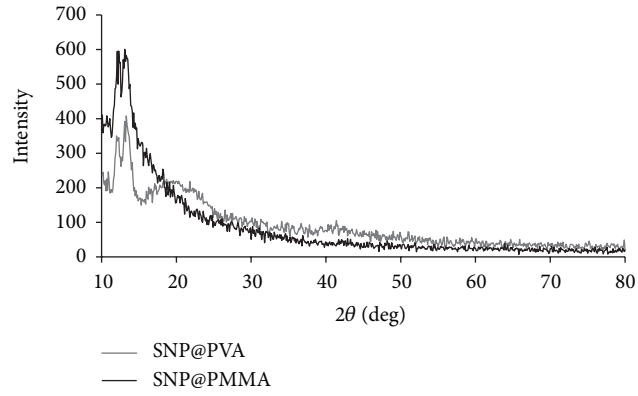

Figure 3: XRD patterns of SNP@PVA and SNP@PMMA films.

Thermal characteristics of the SNP@PVA and SNP@PMMA films were illustrated from the simultaneous TGA/DTA analysis (Figure 6). Thermal analysis of both SNP-polymeric composite films depicted a representative three-stage weight loss profile [23]. The first weight loss

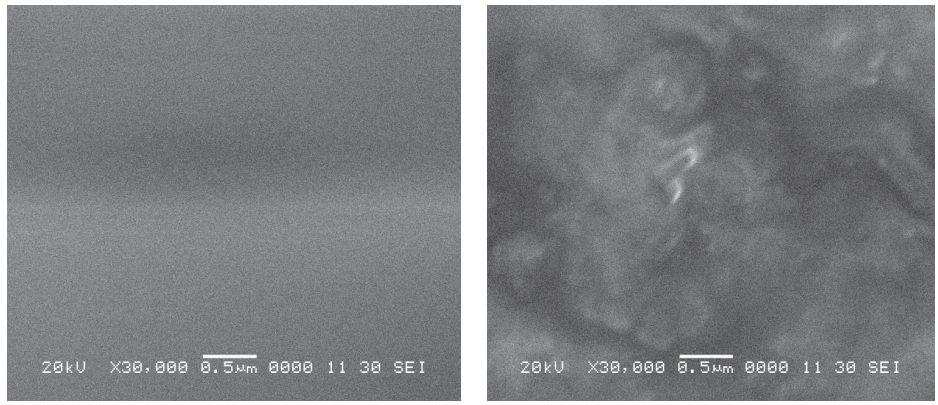

(a) (b)

Figure 4: SEM images of (a) SNP@PVA and (b) SNP@PMMA films.

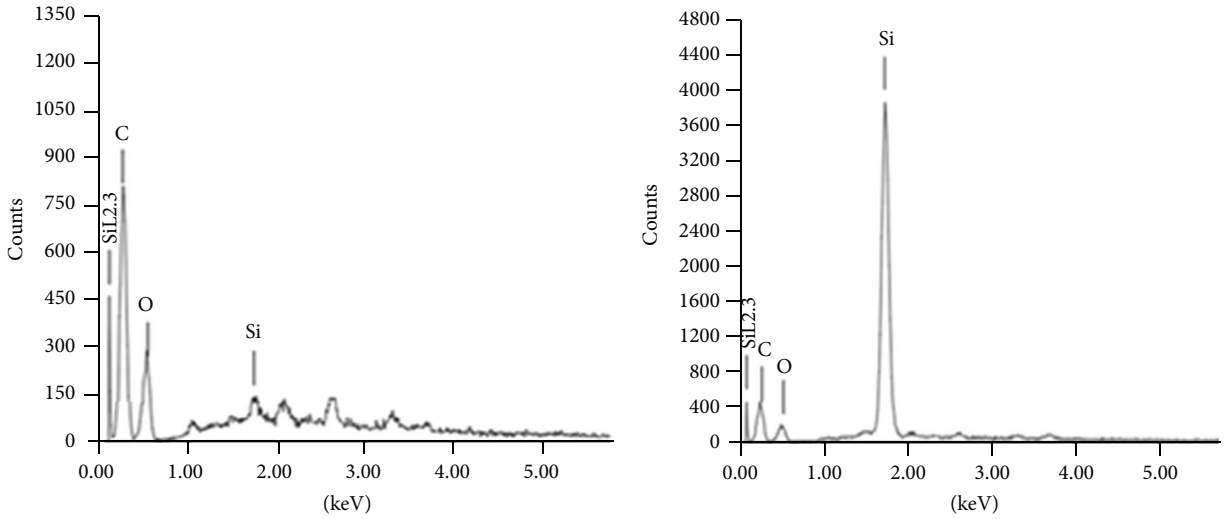

(a) (b)

Figure 5: EDX of (a) SNP@PVA and (b) SNP@PMMA films.

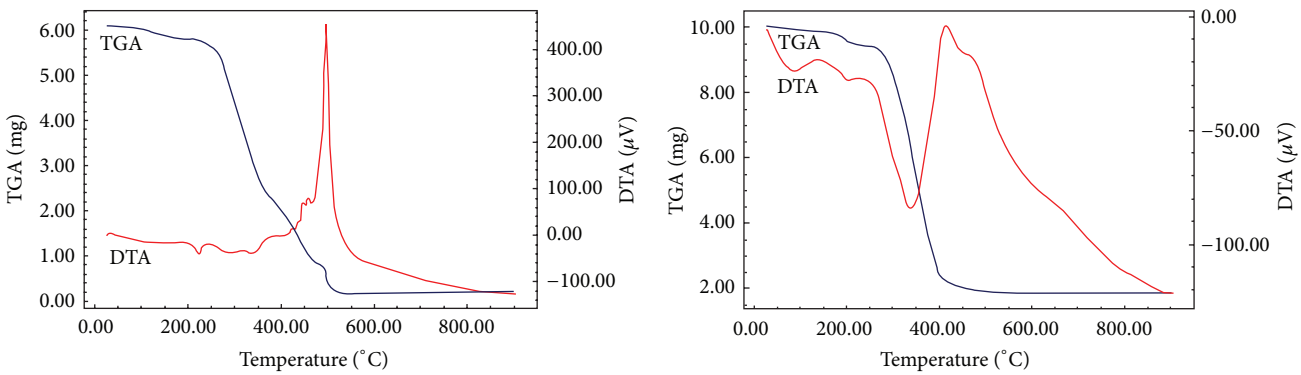

(a) (b)

Figure 6: TGA/DTA of (a) SNP@PVA and (b) SNP@PMMA films.

stage (≈100°C) is associated with the absorbed moisture and volatiles used in preparation of films. The second weight loss stage (≥200°C) is due to initial decomposition of polymers. Subsequent third weight loss stage (≥300°C) corresponds to the complete loss of total organics leaving inorganic residue only.

The SNP@PVA film showed significantly greater weight loss (96.49%) owing to lower SNP content and hence lesser inorganic residue. In case of SNP@PMMA film, weight loss (81.72%) was comparatively less as a result of better interaction involving semicrystalline polymer, PMMA, and SNP. This strong interaction could be attributed to the effective nucleation by SNP, known to facilitate crystallization in PMMA which implied lesser degradation at extreme temperature conditions [24]. Superior thermal resistance of SNP and stronger interactions between the SNP and polymeric matrix enhanced the thermal stability of the SNP-polymeric composite films considerably. These thermostable nanoparticle-polymeric composites would safeguard the packed materials or surfaces against extreme temperature and processing conditions.

SNP@PVA films exhibited significantly higher water retention capacity than SNP@PMMA films (Figure 7) on account of inherent hydrophilic and swelling nature of PVA. The SNP@PMMA films retained less water as a result of their hydrophobic, crystalline, and RGP characteristics [25].

Of the two films tested during *in vitro* antimicrobial study, SNP@PVA film failed to exhibit any significant antimicrobial activity against Gram-positive and Gram-negative bacteria. Hydrophilic nature of PVA caused SNP@PVA film to retain more water and moisture which would incite microbial growth along with physicochemical instability issues. On the contrary, SNP@PMMA film exhibited noteworthy antimicrobial activity against Gram-positive and Gram-negative bacteria, as indicated by areas of inhibition in microbial assays (Figure 8). As a rule, bactericidal mechanism of polymeric composites like PMMA is derived from their destructive interaction with the cell wall and cytoplasmic membranes [26]. Conventionally, inert silica per se was recognized for the absence of significant activity [27]. However, on nanosizing silica, surface-to-volume ratio increased together with enhancement in surface bioactivity of SNP. Besides hydrophobicity, RGP, and crystalline features of SNP@PMMA films initiated bacterial cell phospholipids bilayer penetration [28]. Their antimicrobial performance could be attributed to surface hydrophobic interactions and membrane perforation caused by structural interactions amid PMMA and SNP [29].

Difference in the antibacterial profile of SNP@PMMA film was ascribed to structural variations between Gram-positive and Gram-negative bacteria [30]. Loosely packed outer peptidoglycan layer of Gram-positive bacteria *S. aureus* is known to facilitate deep penetration of the polymeric composites inside the cell to interact with the cytoplasmic membrane. A Gram-negative *E. coli* bacterium has an additional phospholipids bilayer which protects the inner peptidoglycan layer to a greater degree in order to resist the antibacterial activity considerably [31]. Thus, the SNP@PMMA film

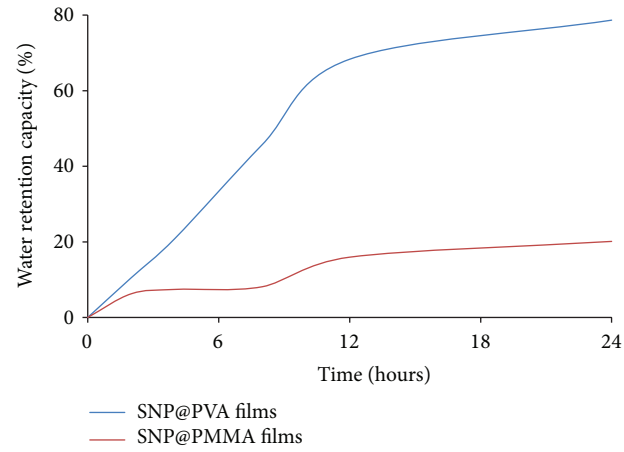

Figure 7: Percent water retention capacity of films.

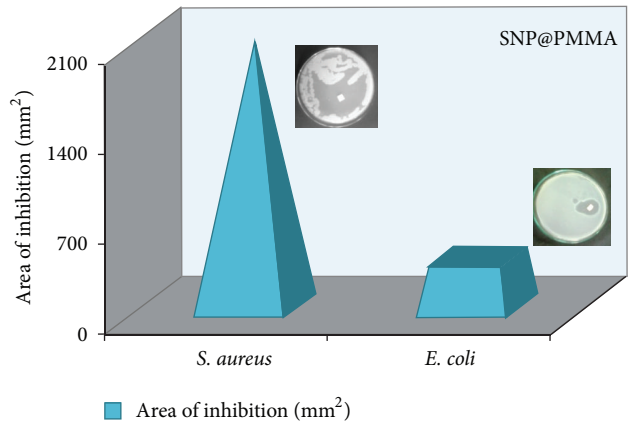

Figure 8: Antimicrobial activity of SNP@PMMA film against *S. aureus* and *E. coli*.

demonstrated maximum inhibitory activity against Gram-positive *S. aureus* compared to Gram-negative bacteria, *E. coli*. Such broad spectrum, active antimicrobial films would prevent degradation of drug formulations and spoilage of food products together with amplification in their stability profile and shelf life. Since no antimicrobial agent or preservative is added, compatibility issues due to their leaching in food or formulation could be outweighed.

4. Conclusions

Silica nanoparticles embedded polymeric (SiO_2 nanoparticles@polymer) composite films were developed and weighed for various traits with feasibility of applications in food, pharmaceutical, and cosmetic industry. Hydrophilic silica nanoparticulate-PVA films showed attributes essential for potential UV filters and thermoresistive materials. Equally, hydrophobic silica nanoparticulate-PMMA films depicted qualities of active, thermostable, antimicrobial materials

which can withstand extreme storage and processing conditions without compromising the shelf life of the drug/food products therein. These nanoparticulate-polymeric composite films can be further explored as sensors, antifouling agents, aseptic fabrics, and implants.

Conflict of Interests

The authors report no conflict of interests regarding the publication of this paper.

Acknowledgment

The authors would like to acknowledge the support and guidance of Dr. G. R. Pathade (Chief Coordinator, Department. of Biotechnology, Fergusson College, Pune).

References

[1] L. Y. Ng, A. W. Mohammad, C. P. Leo, and N. Hilal, "Polymeric membranes incorporated with metal/metal oxide nanoparticles: a comprehensive review," *Desalination*, vol. 308, pp. 15–35, 2010.

[2] A. Rai, A. Prabhune, and C. C. Perry, "Antibiotic mediated synthesis of gold nanoparticles with potent antimicrobial activity and their application in antimicrobial coatings," *Journal of Materials Chemistry*, vol. 20, no. 32, pp. 6789–6798, 2010.

[3] D. Wei, W. Sun, W. Qian, Y. Ye, and X. Ma, "The synthesis of chitosan-based silver nanoparticles and their antibacterial activity," *Carbohydrate Research*, vol. 344, no. 17, pp. 2375–2382, 2009.

[4] H. Dong, J. Huang, R. R. Koepsel, P. Ye, A. J. Russell, and K. Matyjaszewski, "Recyclable antibacterial magnetic nanoparticles grafted with quaternized poly(2-(dimethylamino)ethyl methacrylate) brushes," *Biomacromolecules*, vol. 12, no. 4, pp. 1305–1311, 2011.

[5] M. A. Vargas-Reus, K. Memarzadeh, J. Huang, G. G. Ren, and R. P. Allaker, "Antimicrobial activity of nanoparticulate metal oxides against peri-implantitis pathogens," *International Journal of Antimicrobial Agents*, vol. 40, no. 2, pp. 135–139, 2012.

[6] T. G. Smijs and S. Pavel, "Titanium dioxide and zinc oxide nanoparticles in sunscreens: focus on their safety and effectiveness," *Nanotechnology, Science and Applications*, vol. 4, no. 1, pp. 95–112, 2011.

[7] G. Droval, I. Aranberri, A. Bilbao, L. German, M. Verelst, and J. Dexpert-Ghys, "Antimicrobial activity of nanocomposites: poly(amide) 6 and low density poly(ethylene) filled with zinc oxide," *e-Polymers*, vol. 8, no. 1, pp. 1467–1479, 2008.

[8] O. Girshevitz, Y. Nitzan, and C. N. Sukenik, "Solution-deposited amorphous titanium dioxide on silicone rubber: a conformal, crack-free antibacterial coating," *Chemistry of Materials*, vol. 20, no. 4, pp. 1390–1396, 2008.

[9] L. Vafayi and S. Gharibe, "Investigation of in vitro drug release from porous hollow silica nanospheres prepared of ZnS@SiO_2 core-shell," *Bioinorganic Chemistry and Applications*, vol. 2013, Article ID 541030, 6 pages, 2013.

[10] M. J. Rosemary, I. MacLaren, and T. Pradeep, "Investigations of the antibacterial properties of ciprofloxacin@SiO_2," *Langmuir*, vol. 22, no. 24, pp. 10125–10129, 2006.

[11] B. Gokul, P. Matheswaran, and R. Sathyamoorthy, "Influence of annealing on physical properties of CdO thin films prepared by SILAR method," *Journal of Materials Science & Technology*, vol. 29, no. 1, pp. 17–21, 2013.

[12] H.-J. Jeon, S.-C. Yi, and S.-G. Oh, "Preparation and antibacterial effects of Ag-SiO_2 thin films by sol-gel method," *Biomaterials*, vol. 24, no. 27, pp. 4921–4928, 2003.

[13] A. R. West, *Solid State Chemistry and Its Applications*, John Wiley & Sons, Singapore, 1990.

[14] X. Li, Y. Shen, H. Wang, and G. Fei, "Effects of silica sol on structure and properties of core-shell silicon-acrylic materials," *Advances in Chemical Engineering and Science*, vol. 2, pp. 192–198, 2012.

[15] A. G. Novo, G. Pavlopoulos, and S. T. Feldman, "Corneal topographic changes after refitting polymethylmethacrylate contact lens wearers into rigid gas permeable materials," *The CLAO Journal*, vol. 21, no. 1, pp. 47–51, 1995.

[16] S. Ahmad, S. Ahmad, and S. A. Agnihotry, "Synthesis and characterization of in situ prepared poly (methyl methacrylate) nanocomposites," *Bulletin of Materials Science*, vol. 30, no. 1, pp. 31–35, 2007.

[17] E. F. dos Reis, F. S. Campos, A. P. Lage et al., "Synthesis and characterization of poly (vinyl alcohol) hydrogels and hybrids for rMPB70 protein adsorption," *Materials Research*, vol. 9, no. 2, pp. 185–191, 2006.

[18] S.-T. Hwang, Y.-B. Hahn, K.-S. Nahm, and Y.-S. Lee, "Preparation and characterization of poly(MSMA-co-MMA)-TiO_2/SiO_2 nanocomposites using the colloidal TiO_2/SiO_2 particles via blending method," *Colloids and Surfaces A*, vol. 259, no. 1-3, pp. 63–69, 2005.

[19] Z. Hu, X. Liao, H. Diao, G. Kong, X. Zeng, and Y. Xu, "Amorphous silicon carbide films prepared by H2 diluted silane-methane plasma," *Journal of Crystal Growth*, vol. 264, no. 1-3, pp. 7–12, 2004.

[20] H. Li, H. Deng, and J. Zhao, "Performance research of polyester fabric treated by nano-titanium dioxide (nano-TiO_2) anti-ultraviolet finishing," *International Journal of Chemistry*, vol. 1, pp. 57–60, 2009.

[21] J. F. Lima, R. F. Martins, and O. A. Serra, "Transparent UV-absorbers thin films of zinc oxide: ceria system synthesized via sol-gel process," *Optical Materials*, vol. 35, no. 1, pp. 56–60, 2012.

[22] B. Hatton, L. Mishchenko, S. Davis, K. H. Sandhage, and J. Aizenberg, "Assembly of large-area, highly ordered, crack-free inverse opal films," *Proceedings of the National Academy of Sciences of the United States of America*, vol. 107, no. 23, pp. 10354–10359, 2010.

[23] P. K. Khanna, N. Singh, and S. Charan, "Synthesis of nanoparticles of anatase-TiO_2 and preparation of its optically transparent film in PVA," *Materials Letters*, vol. 61, no. 25, pp. 4725–4730, 2007.

[24] J.-P. He, H.-M. Li, X.-Y. Wang, and Y. Gao, "In situ preparation of poly(ethylene terephthalate)-SiO_2 nanocomposites," *European Polymer Journal*, vol. 42, no. 5, pp. 1128–1134, 2006.

[25] T. V. L. Hima Bindu, M. Vidyavathi, K. Kavitha, T. P. Sastry, and R. V. S. Kumar, "Preparation and evaluation of chitosan-gelatin composite films for wound healing activity," *Trends in Biomaterials and Artificial Organs*, vol. 24, no. 3, pp. 122–130, 2010.

[26] E.-R. Kenawy, F. I. Abdel-Hay, A. E.-R. R. El-Shanshoury, and M. H. El-Newehy, "Biologically active polymers. V. Synthesis and antimicrobial activity of modified poly(glycidyl methacrylate-co-2-hydroxyethyl methacrylate) derivatives with quaternary ammonium and phosphonium salts," *Journal of Polymer Science A*, vol. 40, no. 14, pp. 2384–2393, 2002.

[27] C. H. G. Martins, T. C. Carvalho, M. G. M. Souza et al., "Assessment of antimicrobial effect of Biosilicate against anaerobic, microaerophilic and facultative anaerobic microorganisms," *Journal of Materials Science*, vol. 22, no. 6, pp. 1439–1446, 2011.

[28] D. Das and A. Mukherjee, "Biomaterial film for soluble organic sorption and anti-microbial activity in water environment," *Bioresource Technology*, vol. 110, pp. 412–416, 2012.

[29] L. Qian, H. Xiao, G. Zhao, and B. He, "Synthesis of modified guanidine-based polymers and their antimicrobial activities revealed by AFM and CLSM," *ACS Applied Materials and Interfaces*, vol. 3, no. 6, pp. 1895–1901, 2011.

[30] J. S. Kim, E. Kuk, K. N. Yu et al., "Antimicrobial effects of silver nanoparticles," *Nanomedicine*, vol. 3, no. 1, pp. 95–101, 2007.

[31] A. Munoz-Bonilla and M. Fernández-García, "Polymeric materials with antimicrobial activity," *Progress in Polymer Science*, vol. 37, no. 2, pp. 281–339, 2012.

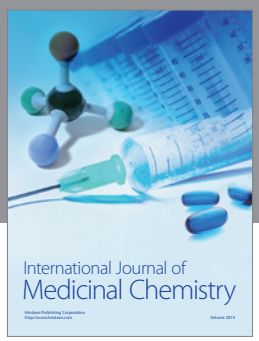

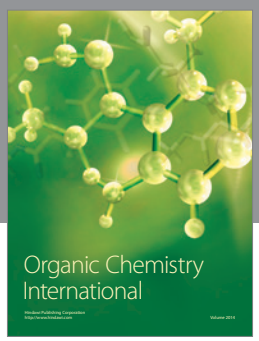

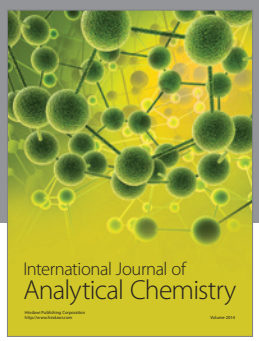

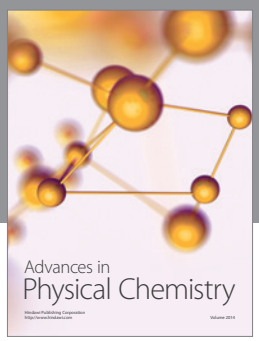

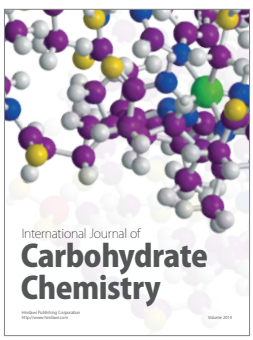

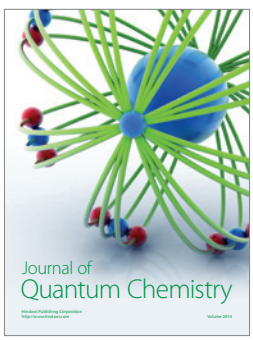

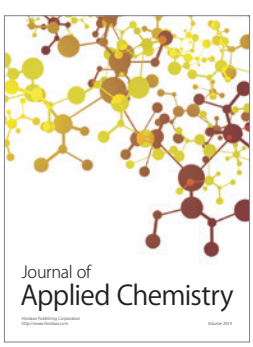

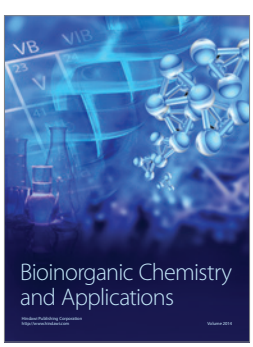

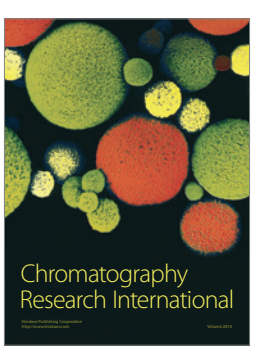

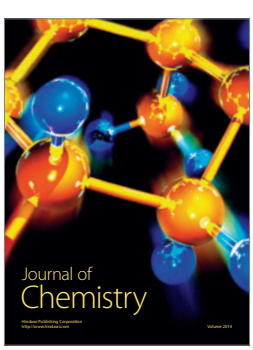

Hindawi

Submit your manuscripts at
http://www.hindawi.com